The Effect of Auger Mechanism on n^+-p GaInAsSb Infrared Photovoltaic Detectors

Yuan Tian, Tianming Zhou, Baolin Zhang, *Member, IEEE*, Hong Jiang, and Yixin Jin

***Abstract*— In this paper, the theoretical analysis of the Auger mechanism in n^+-p GaInAsSb infrared photovoltaic detectors is reported. The lifetime caused by the Auger mechanism is calculated depending on the compositions, temperature, and carrier concentration. We also analyze the effect of material parameters on the detectivity of the n^+-p GaInAsSb detectors. The calculated results show that the Auger mechanism could be suppressed by optimizing the material parameters, so that the performance of GaInAsSb infrared photovoltaic detectors is improved.**

***Index Terms*— Auger mechanism, detectivity, GaInAsSb, infrared photovoltaic detector, (R_0A) product.**

I. Introduction

THE QUATERNARY alloys GaInAsSb create a possibility to fabricate optoelectronic devices for a spectral range of 2–4 μm, which is very important for environmental monitoring and, perhaps in the near future, for optical fiber communication. For example, GaInAsSb alloys have already shown their capabilities to achieve efficient lasers [1] and photodetectors [2], [3].

Until now, most reports have been focused on material fabrication for GaInAsSb detectors [4], [5]. The theoretical analysis of the GaInAsSb detector properties has seldom been considered. In this paper the theoretical calculation and analysis results are discussed for n^+-p $Ga_xIn_{1-x}As_{1-y}Sb_y$ infrared photovoltaic (IR PV) detectors working at room temperature. The figure of merit usually used to characterize the sensitivity of IR PV detectors is the detectivity D^* [6], which is dependent on the quantum efficiency and the zero bias resistance-junction area R_0A product. The influence of diffusion junction current component on the R_0A product and the detectivity of n^+-p $Ga_xIn_{1-x}As_{1-y}Sb_y$ IR PV detectors is considered. Because the lifetime of nonequilibrium carriers is the most important parameter of semiconductor materials, which strongly effects the detector properties, we also discuss the lifetime of Auger recombination in GaInAsSb alloys.

II. Detector Structure and Theoretical Analysis

We consider a generalized detector structure for n^+-$Ga_xIn_{1-x}As_{1-y}Sb_y$/p-$Ga_xIn_{1-x}As_{1-y}Sb_y$/p-GaSb (Fig. 1). Due to the $Ga_xIn_{1-x}As_{1-y}Sb_y$ quaternary alloys lattice-matched to GaSb, the composition x related with the composition y is given by

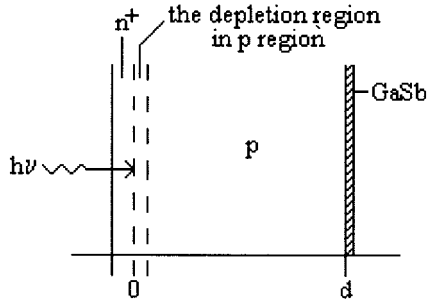

Fig. 1. The detector simple structure.

$$y = \frac{0.408x + 0.022}{0.009x + 0.421}. \tag{1}$$

The detectivity D^* is the main parameter characterizing normalized signal-noise performance of detectors [4]

$$D^* = \frac{\lambda \eta q}{hc}\sqrt{\frac{R_0A}{4KT}}. \tag{2}$$

Two hypotheses are taken into account in (2). One is $\lambda = \lambda_c = hc/Eg$ (Eg is the energy bandgap), and the other is quantum efficiency $\eta = 100\%$. Equation (2) is further simplified by

$$D^* = \frac{q}{Eg}\sqrt{\frac{R_0A}{4KT}}. \tag{3}$$

When the temperature and the composition x and y are fixed, the energy bandgap Eg is kept as a constant, so that the detectivity is only related to the R_0A product. The practical working limit for most IR detectors is a background-limited infrared photodetector (BLIP), in which optical generation resulting from thermal background radiation exceeds the thermal component. The BLIP detectivity is only relative with the temperature and incident optical wavelength [6], [7].

Considering only the diffusion current under a low injection case, in which the diffusion current is caused by the minority-carrier, the R_0A product in the p region is given by [8]

$$(R_0A)_e = \frac{KT}{q^2}\frac{D_ep}{L_en_i^2}\frac{r_esh\left(\frac{d-x_p}{L_e}\right) + ch\left(\frac{d-x_p}{L_e}\right)}{r_ech\left(\frac{d-x_p}{L_e}\right) + sh\left(\frac{d-x_p}{L_e}\right)} \text{ (p-region)}$$

$$D_e = KT\mu_e/q \qquad L_e = \sqrt{D_e\tau_e} \qquad \gamma_e = L_eS_e/D_e. \tag{4}$$

Manuscript received July 16, 1998; revised October 7, 1998. The review of this paper was arranged by Editor P. K. Bhattacharya. This work was supported by the National Advanced Materials Committee of China (NAMCC).

The authors are with the Changchun Institute of Physics, Chinese Academy of Sciences, Changchun 130021, China.

Publisher Item Identifier S 0018-9383(99)02381-3.

The x_p in (4) is the spatial charge of the p region. The D_e, L_e, μ_e, S_e, and τ_e are the diffusion coefficient (cm^2/s), diffusion length (cm), effective mobility ($cm^2/V.s$), and surface recombination velocity (m/s), respectively, for electrons in the p region, and n_i represents the intrinsic carrier concentration (cm^{-3}), and p is the major carrier concentration (cm^{-3}) in the p region. The q and k are electronic charge (C) and Boltzmann's constant ($KeV.K^{-1}$), respectively. The T is the detector working temperature (K).

In (4), $(R_0A)_e$ is embodied by the minority-carrier lifetime, caused by the Auger mechanism. In general, the spatial charge of the p region is much less than that of the quasineutral region, so that the x_p in (4) can be neglected. Thus, (4) and (3) are simplified as

$$(R_0A)_e = \frac{KT}{q^2}\frac{D_e p}{L_e n_i^2}\frac{r_e sh\left(\frac{d}{L_e}\right)+ch\left(\frac{d}{L_e}\right)}{r_e ch\left(\frac{d}{L_e}\right)+sh\left(\frac{d}{L_e}\right)} \tag{5}$$

$$D^* = \frac{q}{Eg}\sqrt{\frac{(R_0A)_e}{4KT}}. \tag{6}$$

Among various types of Auger processes which are possible in an InSb-like band structure, the two with the smallest threshold energy, Auger 1(A-1) and Auger 7(A-7), are most important [9]–[11]. Because the band structure of GaInAsSb quaternary alloys is complicated, it is simplified as an InSb-like band structure in this paper. In the narrow band gap materials, when the spin split-off band is near to or wider than the energy bandgap Eg, the spin split-off band in the Auger mechanism plays a much more important role than A-7 for direct-bandgap materials [14], which is called Auger S(A-S). The A-1 mechanism is dominant in n-type materials, while A-7 and A-S are dominant in p-type materials [12], [13]. Auger mechanism determines the performances of most near-room-temperature PV detectors.

The effective carrier lifetime can be determined by [14]

$$\frac{1}{\tau_A} = \frac{1}{\tau_{A1}} + \frac{1}{\tau_{A7}} + \frac{1}{\tau_{AS}}. \tag{7}$$

The lifetimes for A-1, A-7, and A-S mechanisms are written, respectively, by [14]

$$\tau_{\rm A1} = \frac{2\tau^i_{\rm A1}}{1+n_0/p_0} \tag{8}$$

$$\tau_{\rm A7} = \frac{2\tau^i_{\rm A7}}{1+p_0/n_0} \tag{9}$$

$$\tau_{\rm AS} = \frac{2\tau^i_{\rm AS}}{1+p_0/n_0} \tag{10}$$

where p_0 and n_0 are the hole and electron carrier concentrations at equilibrium state in the same material, respectively, and τ^i indicates the intrinsic reconbination time.

The intrinsic Auger 1 recombination time is given by [12]

$$\tau^i_{\rm A1} = \frac{3.8\times10^{-18}\varepsilon_s(1+\mu)^{1/2}(1+2\mu)\exp\left(\frac{1+2\mu}{1+\mu}\frac{Eg}{KT}\right)}{\frac{m_e^*}{m_0}|F_1F_2|^2\left(\frac{KT}{Eg}\right)^{1/2}} \tag{11}$$

where

- $\mu = m_e^*/m_h^*$ ratio of the conduction and the heavy-hole valence-band effective mass;
- ε_s relative static dielectric constant;
- m_0 electron static mass;
- F_1, F_2 overlap intergrals of the periodic part of the electron wave function.

The intrinsic Auger 7 recombination time is given by [12]

$$\tau^i_{A7} = \gamma\tau^i_{A1} \tag{12}$$

where γ is the ratio of Auger 7 and Auger 1 intrinsic recombination time. According to [10]

$$\gamma = 2\frac{m_e^*(E_{th})}{m_{e0}^*}\frac{1-\frac{5Eg}{4KT}}{1-\frac{3Eg}{2KT}}. \tag{13}$$

The intrinsic Auger S recombination time $\tau^i_{\rm AS}$ shows a different expression for $\Delta > Eg$ as well as $\Delta < Eg$. For $\Delta > Eg$ [15]

$$\tau^i_{\rm AS} = \frac{5\varepsilon m_{hh}^3 m_e^{*(3/2)} KT\Delta^2(Eg+\Delta)\exp\left(\frac{\Delta-Eg}{KT}\right)}{54\pi^4 n_i^2 e^4\hbar^3 m_s^{*(5/2)}(\Delta-Eg)}. \tag{14}$$

For $\Delta < Eg$ [15]

$$\tau^i_{\rm AS} = \frac{\varepsilon^2 m_{hh}^* m_s^{*^2} Eg^5}{2\times18\pi n_i^2 e^4\hbar^3 m_e^*(\Delta+Eg)^2\beta^2[I_1(\beta)-(I_2(\beta)/2]} \tag{15}$$

$$\beta = 2\frac{m_s^*}{m_{hh}^*}\frac{Eg-\Delta}{KT}\frac{Eg^2}{(Eg+\Delta)(3Eg-2\Delta)} \tag{16}$$

$$\begin{aligned} I_1(\beta) = {} & 2\pi^{3/2}\sqrt{\beta}\left[\left(\frac{\pi}{2\sqrt{2}}\right)\int_1^\infty 1-\frac{1}{2t^2}\exp\left(-\frac{\beta t^2}{2}\right)dt\right. \\ & + \int_0^{4/\pi}\sin\theta\exp(-\beta\cos^2\theta) \\ & \left.\cdot\left\{\left[\frac{\theta}{2}-\frac{(\sin 4\theta)}{8}\right]\Big/\cos^2\theta-2\theta\right\}d\theta\right] \end{aligned} \tag{17}$$

$$\begin{aligned} I_2(\beta) = {} & 4\pi\int_0^\infty q^2(4q^2-1)(4q^2+1) \\ & \cdot\left[\left(\frac{4q^2+1}{4q}+\frac{4q}{4q^2+1}\right)\ln\left(\frac{2q+1}{2q-1}\right)^2-2\right] \\ & \cdot\exp\left[-\beta\left(2q^2+\frac{1}{2}\right)\right]dq. \end{aligned} \tag{18}$$

III. Calculation Results and Discussions

In this section, the dependence of the lifetime of the Auger mechanism for GaInAsSb alloys and the detectivity for the n^+-p GaInAsSb detectors on the material parameters are

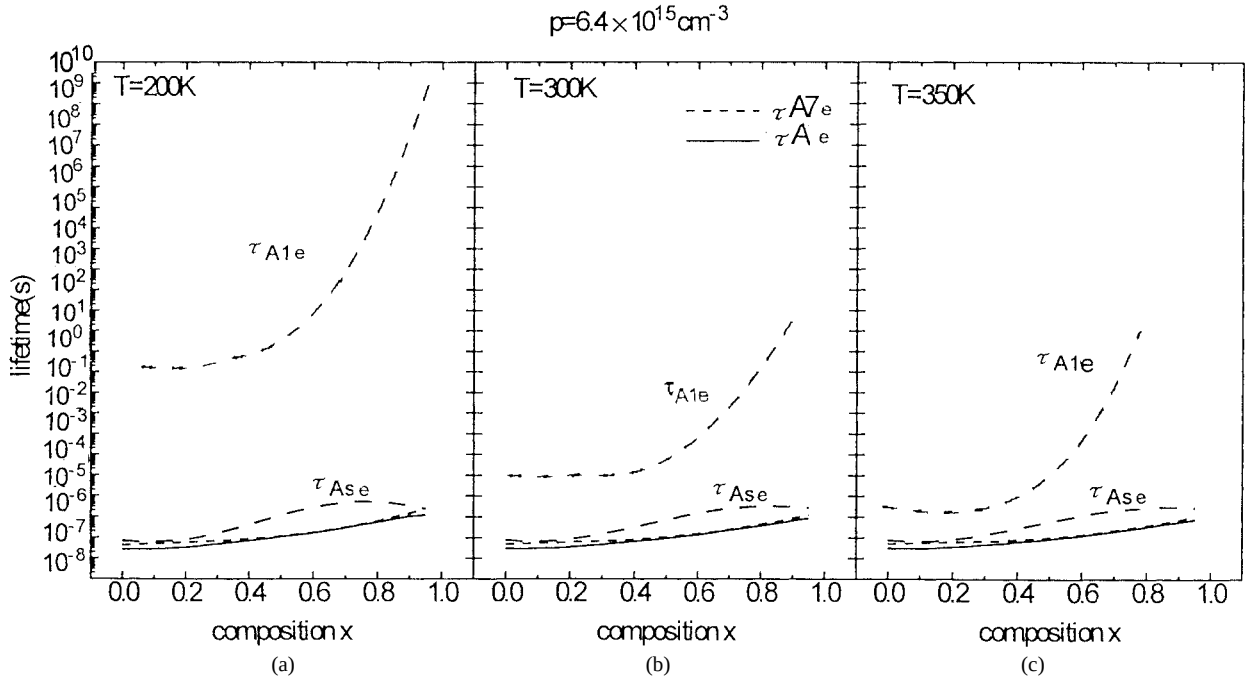

Fig. 2. The dependence of Auger lifetimes on the composition x of p-$Ga_xIn_{1-x}As_{1-y}Sb_y$ alloys lattice-matched to GaSb at different temperatures: (a) $T = 200$ K; (b) $T = 300$ K; (c) $T = 350$ K; for $p = 6.4 \times 10^{15}$ cm^{-3}.

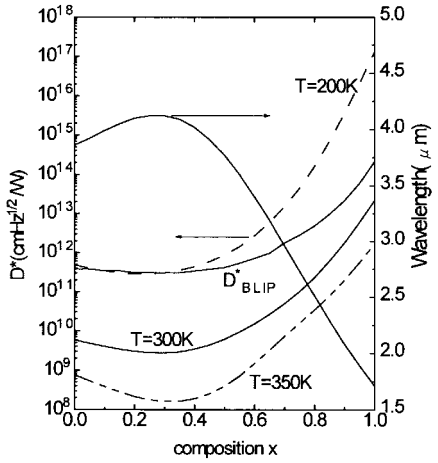

Fig. 3. The dependence of $D^*_{\rm BLIP}$ and the detection wavelength at 300 K and D^* for n^+-$Ga_xIn_{1-x}As_{1-y}Sb_y$ detectors lattice-matched to GaSb at different temperatures on the composition x. $p = 6.4 \times 10^{15}$ cm^{-3}, $\mu_p = 240$ cm^2/v.s, $S_e = 0$, and $d = 5$ μm.

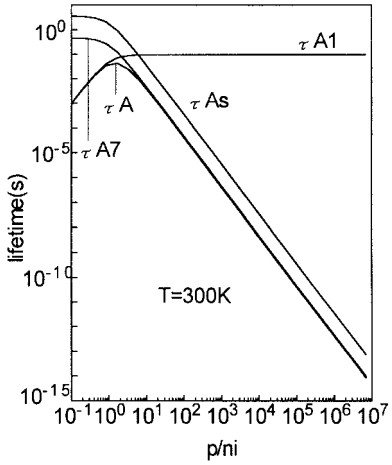

Fig. 4. The Auger lifetimes of a p-$Ga_{0.8}In_{0.2}As_{0.19}Sb_{0.81}$ alloy lattice-matched to GaSb at 300 K as a function of the p-side carrier concentration (p).

analyzed. The dependence of GaInAsSb alloy parameters on the compositions x and y are taken from [16].

The dependence of $\tau_{\rm A1}$, $\tau_{\rm A7}$, and $\tau_{\rm AS}$, $\tau_{\rm A}$ on the composition x in p-$Ga_xIn_{1-x}As_{1-y}Sb_y$ alloys at different temperatures 200, 300, and 350 K is shown in Fig. 2, where the p-side carrier concentration is 6.4×10^{15} cm^{-3}. Fig. 2 indicates that the carrier lifetime strongly depends on Auger 7 and Auger S mechanisms in the p-type materials, and the effect of the Auger 7 process is more apparent in the rich-GaSb range than that in the rich-InAs range.

Fig. 3 shows the dependence of D^* for n^+-p $Ga_xIn_{1-x}As_{1-y}Sb_y$ detectors on the composition x at different temperatures 200, 300, and 350 K. Moreover, $D^*_{\rm BLIP}$ and the detection wavelength at 300 K are plotted in Fig. 3. D^* is calculated from (6), where $p = 6.4 \times 10^{15}$ cm^{-3}, $\mu_p = 240$ cm^2/v.s, $S_e = 0$, and $d = 5$ μm. It is indicated in Fig. 3 that the detectivity will be improved with decreasing the temperature, therefore the extensive detectors cooling is used to improve the performance. However, the cooling makes devices bulky and inconvenient in use. In practice, the suppression of the Auger mechanism is very promising way at the room temperature. Comparing Figs. 2 and 3, the similar trend can be found. The $\tau_{\rm Auger}$ in Fig. 2 and the D^* in Fig. 3 are both increased with composition x. Large $\tau_{\rm Auger}$ suppresses the Auger mechanism so that the performance of detectors is improved, which is expressed as increasing D^*. We hope the detectors work in the range of 2–4 μm, so the rich-GaSb GaInAsSb materials are suitable in Fig. 3. In addition, high D^* can be obtained using these kinds of materials.

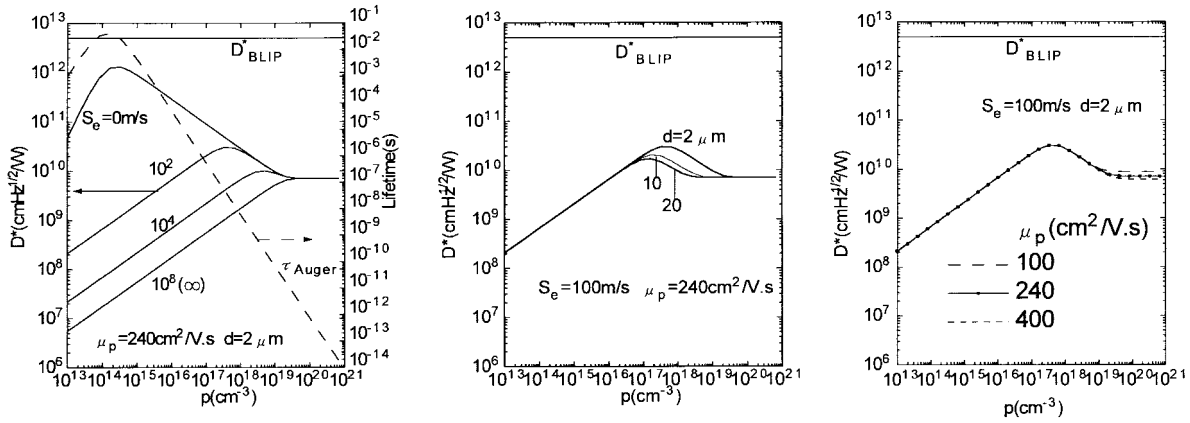

(a) (b) (c)

Fig. 5. The calculated D^* and $\tau_{\rm Auger}$ [Fig. 5(a)] of an n^+-p $Ga_{0.8}In_{0.2}As_{0.19}Sb_{0.81}$ detector latticed-matched to GaSb at 300 K as a function of the p-side carrier concentration (p) and (a) the back surface recombination velocity (S_e); (b) the p-side width (d); and (c) the p-side mobility (μ_p). The BLIP detectivity has been calculated for $T_B = 300$ K and $\eta = 1$.

The dependence of Auger lifetimes in a p-$Ga_{0.8}In_{0.2}As_{0.19}Sb_{0.81}$ alloy on the relative carrier concentration at 300 K is shown in Fig. 4. When the hole carrier concentration is larger than the intrinsic carrier concentration, the probability of holes participating Auger recombination processes higher than that of electrons, thus, Auger 7 recombination becomes the main role and decides the Auger mechanism. Therefore, the influence of the Auger 1 and Auger S processes can be negligible in the range of the carrier concentration larger than the intrinsic carrier concentration. However, in the range near to the intrinsic carrier concentration, all processes will contribute to the carrier lifetime.

Fig. 5 shows the dependence of D^* for an n^+-p $Ga_{0.8}In_{0.2}As_{0.19}Sb_{0.81}$ detector, working at room temperature, on the p-side carrier concentration and other material parameters such as the width (d), the mobility (μ_p), and the back surface recombination velocity (S_e). In addition the $\tau_{\rm Auger}$ as a function of the p-side carrier concentration is plotted in Fig. 5(a) in order to compare how the Auger mechanism effect D^*. Comparing the plots of D^* at $S_e = 0$ and $\tau_{\rm Auger}$ in Fig. 5(a), it is showed that, at $S_e = 0$, high D^* can be obtained with large $\tau_{\rm Auger}$ in the range of $p < 10^{20}$ cm^{-3}. This result also indicates that the suppression of the Auger mechanism can improve D^*. Meanwhile, it is apparent that the higher back surface recombination velocity strongly decreases the detectivity and the peak of D^* moves to the larger carrier concentration with increasing S_e. Until S_e is larger than 10^8 m/s, D^* will not be affected by S_e.

The dependence of the detectivity on the p-side carrier concentration can be divided into three regions. In the range of $p < 10^{16}$ cm^{-3}, only the variation of the back surface recombination velocity has a strong effect on the detectivity, however, in the range of $p > 10^{20}$ cm^{-3}, only the p-side mobility has an influence on the detectivity. In the p-side carrier concentration range of 10^{16}–10^{20} cm^{-3}, variations of all parameters will change the detectivity. Now, let us analyze the above results.

The electron diffusion length in a p-$Ga_{0.8}In_{0.2}As_{0.19}Sb_{0.81}$ alloy is related to the carrier concentration. Table I shows the relationship of the electron diffusion length with p-side carrier concentration with $\mu_p = 240$ cm^2/V.s and $T = 300$ K. Using Table I, (5) can be made a further approximation basing on the relationship of L_e and d.

TABLE I
THE RELATIONSHIP OF THE ELECTRON DIFFUSION LENGTH WITH THE p-SIDE CARRIER CONCENTRATION

p-side carrier concentration(p) (cm^{-3})	Electron diffusion length in p region(Le) (μm)
$p<10^{16}$	$Le>10^2$
$10^{16}<p<10^{20}$	$10^{-2}<Le<10^2$
$p>10^{20}$	$Le<10^{-2}$

For $d \gg L_e (p > 10^{20}$ cm$^{-3})$

$$(R_0A)_e = \frac{KTp\tau_e}{q^2n_i^2L_e} = \frac{1}{qn_i^2}\sqrt{\frac{KT}{q\mu_e}}\sqrt{p^2\tau_e}. \tag{19}$$

For $d \ll L_e (p < 10^{16}$ cm$^{-3})$

$$(R_0A)_e = \frac{KTp}{q^2n_i^2}\frac{L_e}{D_e}\frac{r_e\dfrac{d}{L_e}+1}{r_e+\dfrac{d}{L_e}} \tag{20}$$

if d/L_e is neglected in (20),

$$(R_0A)_e = \frac{KTp}{q^2n_i^2S_e}. \tag{21}$$

For $d \sim L_e (10^{16} < p < 10^{20}$ cm$^{-3})$, it is just (5).

Equations (21), (19), and (5) correspond to the above three regions. For $d \ll L_e$, $(R_0A)_e$ is not related with the width and the mobility, while $(R_0A)_e$ is not related with S_e and d for $d \gg L_e$. Because of $D^* \sim \sqrt{(R_0A)_e}$ in (6), the variation of D^* is similar to that of $(R_0A)_e$.

A common characteristic exists in each part of Fig. 5. When the p-side carrier concentration is larger than 10^{20} cm$^{-3} (d \gg L_e)$, the detectivity stays a constant with increasing p-side carrier concentration, with μ_p as a constant. This result can be explained from (19).

Substituting (8), (9), and (10) into (7), we can obtain

$$p^2\tau_e = \frac{1}{1+ni^2/p^2} \times \frac{2ni^2}{\tau^i_{\rm A1}ni^2/p^2 + 1/\tau^i_{\rm A7} + 1/\tau^i_{\rm AS}}. \quad (22)$$

Because of $p \gg ni (p > 10^{20}$ cm$^{-3})$, the relationship of $ni^2/p^2 = 0$ can be used, thus

$$p^2\tau_e = \frac{2ni^2}{1/\tau^i_{\rm A7} + 1/\tau^i_{\rm AS}}. \quad (23)$$

For a fixed composition x and temperature, $p^2\tau_e$ is kept as a constant. Due to $(R_0A)_e \sim \sqrt{P^2\tau_e}$ in (21), $(R_0A)_e$ is a constant with a fixed μ_p. In (6), $D^* \sim \sqrt{(R_0A)_e}$, D^* is kept as a constant for $p > 10^{20}$ cm^{-3} with a fixed μ_p, which has been shown in Fig. 5. This result also indicates that the Auger mechanism will not affect the detectivity when the p-side carrier concentration is larger than 10^{20} cm^{-3}.

IV. Conclusions

In this paper, the theoretical analysis of the Auger mechanism influence on the n$^+$-p GaInAsSb infrared photovoltiac detectors is considered. It is shown that the Auger mechanism is embodied through the lifetime which depends on the material carrier concentration. The detectivity D^* is affected by the Auger mechanism when the carrier concentration in the p region is less than 10^{20} cm^{-3}. At the same time, the calculated results demonstrates that reducing the volume and the carrier mobility in the p region will increase the corresponding detectivity. Under the condition of the thin p region ($d \ll L_e$), the lower surface recombination velocity is expected for in an n$^+$-p structure.

References

[1] H. K. Choi and S. J. Eglash, "Room-temperature CW operation at 2.2 μm of GaInAsSb/AlGaAsSb diode lasers grown by molecular beam epitaxy," *Appl. Phys. Lett.*, vol. 59, no. 10, pp. 1165–1169, 1991.

[2] B. Zhang, T. Zhou, H. Jiang, Y. Ning, and Y. Jin, "GaInAsSb infrared photodetectors prepared by MOCVD," *Electron. Lett.*, vol. 31, no. 10, pp. 830–832, 1995.

[3] B. Zhang, Y. Jin, T. Zhou, H. Jiang, Y. Ning, and S. Li, "The properties of GaInAsSb/GaSb heterostructure grown by MOCVD and p-GaInAsSb/n-GaSb photodiodes," in *Proc. Mater. Res. Soc. Symp.*, 1996, vol. 415, pp. 31–26.

[4] M. Mebarki and D. Boukredimi, "Electrical determination of band offsets in a p-$Ga_{0.77}In_{0.23}As_{0.2}Sb_{0.8}$/n-GaSb type II heterojuction," *J. Appl. Phys.*, vol. 73, no. 5, pp. 2360–2369, 1993.

[5] M. P. Mikhaillova and A. N. Titkov, "Type II heterojunctions in the GaInAsSb/GaSb system," *Semicond. Sci. Technol.*, vol. 9, pp. 1279–1295, 1994.

[6] M. B. Reine, A. K. Sood, and T. J. Tredwell, "Photovoltaic infrared detector," *Semiconductors and Semimetals*, vol. 18, R. K. Willardson and A. C. Beer, Eds. New York: Academic, 1981, ch. 6. p. 237.

[7] J. Piotrowski, W. Gawron, and Z. Djuric, "New generation of near room temperature photodetectors," *Opt. Eng.*, vol. 33, no. 5, pp. 1413–1421, 1994.

[8] A. Rogalski and J. Rutkowski, "Effect of structure on the quantum efficicncy and R_0A product of lead–tin chalcogenide photodiodes," *Infrared Phys.*, vol. 22, no. 2, pp. 199–208, 1982.

[9] P. E. Peterson, "Auger recombination in mercury cadmium telluride," *Semicoductors and Semimetals*, vol. 18, R. K. Willardson and A. C. Beer, Eds. New York: Academic, 1981, ch. 4, pp. 121–155.

[10] T. N. Cassalman and P. E. Peterson, "A comparison of the dominant Auger transition in p-type (Hg, Cd)Te," *Solid State Commum.*, vol. 33, no. 6, pp. 615–619, 1980.

[11] T. N. Cassalman, "Calculation of the Auger lifetime in p-type $Hg_{1-x}Cd_xTe$," *J. Appl. Phys.*, vol. 52, no. 2, pp. 848–854, 1981.

[12] M. Takeshima, "Auger recombination in InAs, GaSb InP and GaAs," *J. Appl. Phys.*, vol. 43, no. 10, pp. 4114–4118, 1972.

[13] A. R. Beattie and G. Smith, "Recombination in semiconductors by a light hole Auger transition," *Physica Status Solid*, vol. 19, no. 2, pp. 577–586, 1967.

[14] A. Rogalski and Z. Orman, "Band-to-band recombination in $InAs_{1-x}Sb_x$," *Infrared Phys.*, vol. 25, no. 3, pp. 551–560, 1985.

[15] B. L. Gelmont, "Auger recombination in diamond-like narrow-gap semiconductors," *Phys. Lett., A* vol. 66, no. 4, pp. 323–324, 1978.

[16] Y. Tian, T. Zhou, B. Zhang, and Y. Jin, "Theoretical analysis of Auger mechanism in a GaInAsSb infrared photovoltaic detector," *Opt. Eng.*, vol. 37, no. 6, pp. 1754–1762, 1998.

Yuan Tian was born in Fushun, China. She received the B.S. degree in physics from Jilin University, Changchun, China, in 1994. She is currently pursuing the M.S. and Ph.D. degrees on program for semiconductor photo-electronic materials and devices at Changchun Institute of Physics, Chinese Academy of Sciences, Changchun.

Tianming Zhou received the B.S. degree in physics from the University of Science and Technology of China, Hefei, in 1964.

Since 1964, he has been a Researcher at Changchun Institute of Physics, Chinese Academy of Sciences, Changchun, where he has worked on the growth of semiconductor materials and the research of optoelectronic devices. His current research interests include the growth and characterization of narrow bandgap III–V compounds and infrared optoelectronic devices.

Baolin Zhang (M'97) received the M.S. degree in semiconductor physics and devices from Jilin University, Changchun, China, in 1989.

He is currently a Researcher at Changchun Institute of Physics, Chinese Academy of Sciences, Changchun. His current research interests include the growth and characterization of III–V compounds via metalorganic vapor phase (MOVPE) technique and luminescence from silicon and opto-electronic devices based on silicon materials.

Hong Jiang received the B.S. degree from the Department of Electrical Science, Jilin University, Changchun, China, in 1986.

Since 1986, she has been with the Changchun Institute of Physics, Chinese Academy of Sciences. Changchum, where she has been working in the field of compound semiconductors, especially MOCVD growth of III–V compounds.

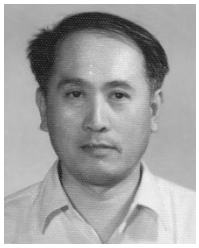

Yixin Jin received the B.S. degree from the Department of Physics, Peking University, Peking, China, in 1965, and the degree of Docteur de L'Universte en Sciences, from the Universite des Sciences et Techniques du Languedoc, France, in 1981.

Since 1965, he has been with Changchun Institute of Physics, Chinese Academy of Sciences, Changchun. From 1979 to 1981, he was with the Center Des Electroniques des Solides, Universite des Sciences et Techniques du Languedoc, France. His research field covers the luminescence materials and physics, preparation and characterization of optoelectronic materials, and functional materials. His current research interest is the materials in photonics.